Volume 256, number 1,2, 4–10 FEB 07668 October 1989

The number of molecules taken up by electroporated cells: quantitative determination

David C. Bartoletti, Gail I. Harrison and James C. Weaver

Harvard-M.I.T. Division of Health Sciences and Technology, Massachusetts Institute of Technology, Cambridge, MA 02139, USA

Received 10 July 1989

Fluorescent and fluorescent-labeled molecules were used with calibrated flow cytometric fluorescence measurements of electrically pulsed cells (intact yeast: *Saccharomyces cerevisiae*) to demonstrate a method for determining the net number of molecules transported into electroporated cells. For the conditions used, a single pulse of width 50 μs and magnitude 8.0 ± 0.5 kV/cm resulted in an average net molecular uptake which is large, $\bar{n} = 1.4 \times 10^5$ molecules of 70 kDa FITC-dextran (supplied extracellular concentration of 500 μM), and $\bar{n} = 1.0 \times 10^8$ molecules of 660 Da propidium iodide (PI; 80 μM). Both molecules were present in pulsed cells at less than equilibrium values, consistent with a transient uptake mechanism. Intracellular FITC-dextran is present in soluble form, while PI is predominantly bound to nucleic acids. A broad, statistically significant distribution of molecular uptake was also observed. Such quantitative determinations should be important for guiding applications of electroporation, and for testing models of electroporation mechanisms. Further, the use of PI, which is well established as a membrane exclusion dye, provides additional support for the interpretation that both PI and FITC-dextran were internalized as a result of an electrical pulse.

Electroporation; Molecular transport; Number of molecules; Flow cytometry; Yeast

1. INTRODUCTION

An applied electric field, $E(t)_e$, causes an elevated transmembrane potential, $U(t)$, of cell membranes. As used here, 'electroporation' indicates the occurrence of transient pores in a membrane due to a large $U(t)$ [1,2]. Although their shapes and sizes are not actually known, the pores are believed to provide aqueous pathways for the movement of both ions and molecules. There are many consequences of the pores, including (i) reversible electrical breakdown (REB) at large $U(t)$, which rapidly discharges the membrane, (ii) rupture due to moderately elevated $U(t)$, and (iii) transport of molecules by mechanisms which may include permeation, electrokinetic transport, and hydrodynamic flow due to an osmotic pressure difference through a population of time varying pores. Previous studies which determined molecular uptake or release have emphasized measurements on total cell populations, but have not determined the numbers of the transported molecules [3–5]. Similarly, imaging based studies which have focused on the kinetics and the sites of transport in an individual cell have not been presented in terms of quantitative molecular transport [6,7].

Quantitation determinations of the numbers of transported molecules should be important in guiding applications of electroporation. Recently many reports have described the use of electroporation for DNA transfer, but without knowledge of the actual amount of molecular uptake [1,2,8]. In those procedures 'success' is scored by counting the eventual number of transformed cells, i.e. by scoring a biological endpoint far removed from electroporative uptake. If a cell is transformed, following electroporative uptake

Correspondence address: J.C. Weaver, 20A-128, MIT, Cambridge, MA 02139, USA

Published by Elsevier Science Publishers B.V. (Biomedical Division)

several intracellular processes must all be successful: the internalized DNA must be transported through the cytoplasm without degradation, transported into the nucleus, integrated into the host DNA, and then expressed. If the number of initially internalized DNA fragments were known, it would be possible to determine whether small transformation frequencies are due to small amounts of uptake, or are instead due to unsuccessful completion of the intracellular processes, and strategies for improvement might be pursued.

Similarly, in order to understand molecular transport mechanisms associated with electroporation, determination of the number of molecules which cross the membrane is essential. Quantitative measurements of the net number of transported molecules of various sizes, shapes and charge will provide data for testing models of electroporative transport. For example, models which involve a population of time varying pores may describe the time-dependent membrane transport processes through the pores. The same models may provide a quantitative description of pore shrinkage kinetics, and this should allow membrane recovery to be described. During recovery the molecular exclusion is expected to continuously change, progressing to smaller molecular cutoffs. As illustrated here, it should be possible to carry out molecular transport measurements for testing models and for guiding applications.

Previous studies have measured molecular transport effects due to a large number of cells, using methods such as turbidity changes [3], total enzymatic activity [9], or radioactive isotope uptake [4,5], in a cell or vesicle population. Important information was obtained from the average behavior of the cell population, but could not reveal variations in electroporation behavior of the individual cells within the population. Others have focused on individual cell measurements. Several important studies have emphasized kinetic studies using individual cells, examining the uptake or release of fluorescent molecules by video image analysis [6,7]. Important information regarding the sites and time dependence of transport was obtained. However, experiments of this type are subject to the limitation that because one or a small number of individual cells are studied, the cells may not be representative. A complementary approach is based on the use of flow cytometry to individually measure large numbers (e.g. 10^4) of cells, and to determine the net uptake or release of each. However, this type of experiment is subject to the limitation that rapid molecular transport kinetics cannot be readily studied. In all of these methods it should be possible to carry out calibrations so that the resulting data can be interpreted in terms of the numbers of molecules which cross the cell membrane. Here we have illustrated a method which involves flow cytometry for quantitative measurements of large numbers of individual cells, but with fluorescence measurements calibrated in terms of numbers of molecules by spectrofluorometry. Impressively large numbers of molecules are found to be taken up by individual cells.

2. MATERIALS AND METHODS

Two different molecules, one with 'green fluorescence' (GF; FITC-dextran; 70 kDa; Sigma) and the other with 'red fluorescence' (RF; propidium iodide = PI; 660 Da) were used separately, so that an individual experiment involved either GF or RF measurement, but not both. This is in contrast to an earlier, related study in which FITC-dextran was present while cells were pulsed, and the cells were then exposed to PI 25 min after the pulse [10]. Here either the GF or RF fluorescent molecule was provided at the time of application of a single, 50 μs square wave pulse of amplitude E_e = 8.0 ± 0.5 kV/cm, and time was allowed for membrane recovery before measurement. In the case of FITC-dextran, a recovery period of 5 min was provided before cells were washed (centrifuged at 4500 × g for 3 min). In the case of PI the cells were initially suspended in a 80 μM solution, pulsed and allowed to recover for 5 min, but no washing was provided. The RF emission of PI is well known to increase significantly as PI binds to doubly stranded nucleic acids, which requires that PI be kept in solution in order to maintain significant equilibrium binding [11]. The protocols and conditions are otherwise the same as those used previously with the same intact microorganism, *Saccharomyces cerevisiae*, grown and harvested under the same conditions [10]. For this reason, tests of viability based on plating were not repeated here, nor was there any attempt to assess membrane recovery after the pulse. Instead, the entire emphasis was on determining the net number of molecules taken up under the same conditions (suspension medium, pH, pulse characteristics, chamber and electrode type and spacing) used previously.

The first set of experiments focused on the uptake of the macromolecule FITC-dextran. The GF of individual cells was measured as reported previously [10], but with calibration which allowed GF measurements to be interpreted in terms of numbers of FITC-dextran molecules. The calibration was carried out using two different methods: first by seeking a calibration based on the fluorescence of serial dilutions of FITC-dextran using a spectrofluorometer (Fluorolog F111AI, SPEX Industries), and second by directly calibrating the flow cytometer with fluorescent beads (4.4–9.0 μm diameter, Flow

Cytometry Standards Corp., Research Triangle Park, NC). There was difficulty with the first method, which we attribute to loss of unknown amounts of FITC-dextran from the cells during a filtration/wash step after centrifugation. For this reason we used standardized fluorescent beads to calibrate GF measurements. The fluorescent beads were labeled with a known number of equivalent soluble fluorescein (ESF) molecules, which provided the basis for calibrating the flow cytometer GF channel in terms of ESF molecules [12]. Beads at a concentration of 4.5×10^5 beads/ml in phosphate buffer at pH 6.8 were passed through the flow cytometer with RBS (right angle blue scatter) used as a trigger signal. The GF calibration in terms of ESF was converted to an equivalent number of FITC-dextran molecules by using the average labeling density (number of FITC groups per FITC-dextran) determined by us using the spectrofluorimeter. Different dextran lots were found to range from about 3–15 fluorescein labels (in the isothiocyanate form) per 70 kDa dextran. For the uptake experiments we used dextran with 3.9 FITC labels per 70 kDa FITC-dextran.

We verified that one ESF yields the same fluorescence intensity as one FITC label. First, using the spectrofluorimeter the emission spectra for beads and FITC-dextran were recorded and found to be nearly identical from 515 to 530 nm. Second, the GF emission of a bead suspension of known bead concentration was compared to the GF emission of a known solution of FITC-dextran which contained non-fluorescent beads at known bead concentrations. This was a necessary precaution, as beads affect both absorption and light scattering, and can alter both fluorescence excitation and fluorescence emission intensities. The same optical volume, V_{opt}, within the spectrofluorimeter was used in all cases, so that the relationship n_{FITC}/n_{ESF} = [FITC-dextran] · V_{opt} · $Label_{dextran}$/([bead] · V_{opt} · $Label_{bead}$) = $I_{GF,dextran}/I_{GF,bead}$ could be used to relate the two emission intensities, $I_{GF,dextran}$ and $I_{GF,bead}$, and thereby to obtain the calibration between fluorescent beads and FITC-dextran. Here $Label_{dextran}$ is the number of FITC labels per 70 kDa dextran, and $Label_{bead}$ is the number of ESF per bead. We estimate the calibration error to be about 10%. Considering the actual variation in uptake (see figures), this is sufficiently accurate.

Cells were pulsed as previously described [10], using E_e = 8.0 ± 0.5 kV/cm, and the GF cell distribution (a histogram) was computed in terms of the number of FITC-dextran molecules. As in the previous study, we interpret the resulting cellular GF as due to uptake of FITC-dextran. There is no evidence by fluorescence microscopy of a bright fluorescent rim (which would indicate significant surface binding rather than a homogeneous intracellular distribution of FITC-dextran). Further, the interpretation that PI is internalized under the same electroporation conditions is compelling (see below).

The flow cytometer detection limit for FITC-dextran under our conditions was estimated by making GF measurements with non-fluorescent beads, as even non-fluorescent particles exposed to the flow cytometer's intense 488 nm excitation gave rise to a small GF signal because of incomplete rejection of the 488 nm light. In addition, noise events in the GF channel contribute to a GF detection limit. Finally, any small spontaneous cell surface adsorption will contribute. The net result was the GF detection limit obtained from the unpulsed cell GF histogram (fig.2a) which had a mean GF value corresponding to 1.8×10^4 ESF. This bead measurement is equivalent to a detection limit of 4.6×10^3 FITC-dextran molecules for the highly scattering beads. The same measurement made wi' cells (smaller light scattering) is about 1×10^3 FITC-dextran molecules (fig.2a), far less than the uptake due to electroporation.

The second set of experiments used propidium iodide (PI), which is polar, much smaller, and widely used as membrane-exclusion dye [11,13]. Here we exploited PI's inability to penetrate intact cell membranes, and the increase of RF which occurs upon binding of PI to doubly stranded nucleic acids (fig.1). There is, however, an important difference compared to our previous use of PI to partially test for membrane recovery, wherein we first exposed cells to PI 25 min after a pulse [10].

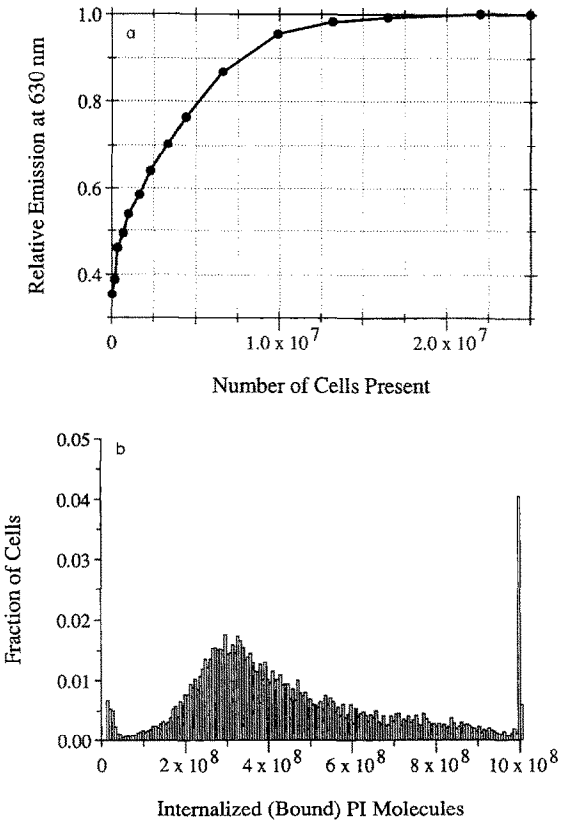

Fig.1. (a) Change in 'red fluorescence' (RF; emission at 630 nm) of propidium iodide (PI) as the number of methanol-fixed yeast cells is increased for a constant amount of PI. The fixed cells provide readily accessible binding sites for PI in the form of doubly stranded nucleic acids. The provided PI concentration was 5 μM, which is significantly less than the 80 μM used with electrically pulsed cells. (b) Population distribution of the number of PI molecules bound to fixed yeast exposed to a 80 μM concentration. The computed average of this flow cytometer distribution is compared with the spectrofluorimeter measurement (fundamentally an average) in order to provide an appropriate calibration.

Here PI was present at the time of the pulse, and was maintained during flow cytometer measurements.

A different calibration process was used for PI because calibration of nucleic acid bound PI (rather than soluble PI) was needed. The bound PI calibration was obtained by first providing soluble 5 μM PI in the spectrofluorometer, with excitation at 488 nm, and RF measured at 630 ± 2.25 nm. Known numbers of cells fixed in 50% methanol, grown under the same conditions as the electrically pulsed cells, were added stepwise to the cuvette to provide increasing numbers of readily accessible nucleic acid-binding sites, and the increase in RF emission was determined (fig.1). At each addition of cells, the RF of the same concentration of cells with no PI present was measured to correct the data for light scattering and absorbance. The RF rises until approx. 2×10^7 cells have been added (fig.1), at which point we assumed that essentially all PI was bound. Using a PI concentration of 5 μM, we determined that there was an average binding of $\bar{n} = 4.5 \times 10^8$ molecules per methanol-fixed cell. This allowed us to use a large number of fixed cells, which were equilibrated with 5 μM PI in the flow cytometer sample stream, to be used as a transfer standard. Specifically, separate measurement and analysis of fixed and of electrically pulsed cells allowed us to determine the amount of RF of individual pulsed cells relative to the average RF of the fixed cells, and this in turn allowed us to determine the number of PI molecules which entered a pulsed cell and then bound to some of the large number of nucleic acid molecules within the cell.

The RF flow cytometer measurements of pulsed cells were interpreted as internalized, nucleic acid-bound PI for two reasons. First, PI is widely used as a membrane integrity probe, for which it is well established that significant RF occurs only when PI enters a cell with a permeabilized membrane and then binds to double-stranded intracellular nucleic acids [11,13]. We confirmed (fig.1) that the RF of PI rises significantly upon nucleic acid binding in fixed cells using the conditions of our experiments. Second, we observed no bright fluorescent rim, indicating that no significant surface binding occurred.

3. RESULTS AND DISCUSSION

Previously [10], it was found that there were significant population distributions of the fluorescence of pulsed yeast cells, using the same macromolecule (FITC-dextran; 70 kDa) for uptake assessment as in the present study. However, PI was used there as a partial indicator of membrane recovery, by exposing cells to PI 25 min after an electrical pulse. In contrast, the present study uses PI in the same manner as FITC-dextran. That is, either FITC-dextran or PI is provided at the time of a pulse, a time for recovery is allowed, and then the cells are measured individually by flow cytometry. As in the prior study, intact *S. cerevisiae* cells were exposed to a single 50 μs duration pulse of amplitude $E_e = 8.0 \pm 0.5$ kV/cm, an electrical pulse condition close to that then found to result in the maximum percentage of cells exhibiting significant FITC-dextran uptake. As before, we emphasize that E_e is the actual electric field believed to exist within the electrolyte of the cell suspension while the pulse is on, and is not the nominal electric field computed simply by dividing the applied potential difference by the planar electrode spacing [10].

The previous studies focused on the percent of participating cells, i.e. the percent that took up a measurably large amount of FITC-dextran, whereas the present study focused on the actual number of molecules taken up by each cell within a large population of pulsed cells. The population distribution of net molecular uptake was then displayed in the form of a histogram, i.e. a plot of the frequency-of-occurrence vs the amount of uptake. As shown in fig.2, the average cell with significant GF has taken up $\bar{n}_{\text{FITC-dextran}} = 1.4 \times 10^5$ molecules of FITC-dextran. This is a large number. Further, there is a wide distribution around this mean value. If 10% to 90% limits are somewhat arbitrarily used to indicate the width of the distribution, the individual cell uptake can be characterized as $\bar{n}^{+\Delta n10\%}_{-\Delta n90\%} = 1.4^{+1.0}_{-1.28} \times 10^5$ molecules. The ± limits are not errors, but instead a compact, partial representation of a true variation within the cell population.

The effective average concentration, $\bar{C}_{\text{int}}$, of internalized FITC-dextran was estimated by computing the number of molecules per average cell volume, $\bar{V}_{\text{cell}}$, which is of the order of 10^{-10} cm^{-3}. $\bar{C}_{\text{int}}$ was found to be of the order of 10^{-6} M, which is much less than 1% of the extracellular concentration. Thus, the $\bar{C}_{\text{int}}$ was far less than the equilibrium value of 5×10^{-4} M, which is consistent with a transient transport mechanism. Further, because of the magnitude of $\bar{C}_{\text{int}}$ insignificant quenching of fluorescence should have occurred, and therefore the calibrated GF measurements provided reasonable estimates of molecular uptake. Finally, we note that in future extensions of the present approach, the volume of each cell might be individually measured simultaneously by use of 'negative fluorescence' [15], using another fluorescence 'color' which labels a very large macromolecule which is supplied in solution following a membrane recovery period. This would provide the basis for more accurately estimating the intracellular concentration of molecules taken up because of electroporation.

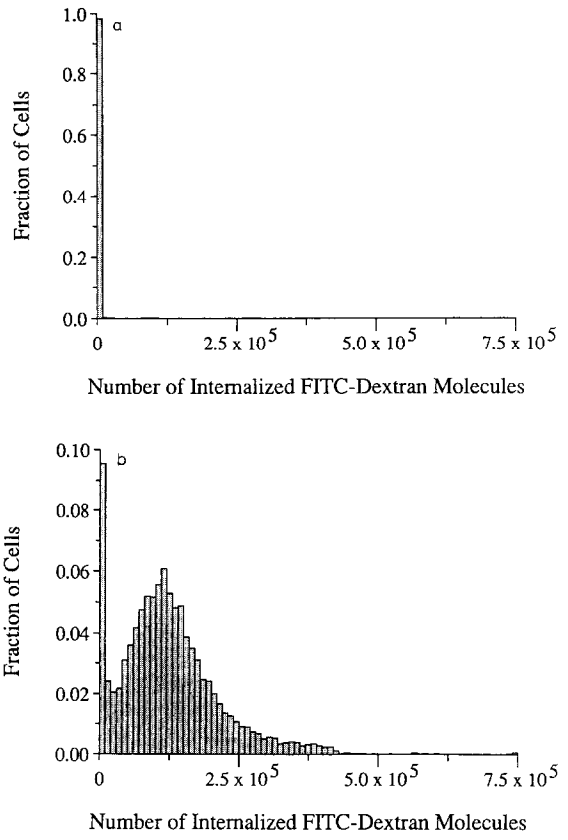

Fig.2. (a) Control distribution of GF (presented in terms of equivalent numbers of FITC-dextran molecules) obtained with non-pulsed cells exposed to FITC-dextran at a concentration of 500 μM. The average control GF signal corresponds to about 1×10^3 molecules per cell, which is much lower than for pulsed cells. (b) Population distribution of the number of FITC-dextran molecules taken up by pulsed cells exposed to 500 μM FITC-dextran. The cells were subjected to a single 50 μs pulse of amplitude $E_e = 8.0 \pm 0.5$ kV/cm. The average of this distribution corresponds to $\bar{n}_{\text{FITC-dextran}} = 1.4 \times 10^5$ molecules of FITC-dextran. The wide distribution around this mean value is clearly indicated by the graphical display. A less complete, but compact description of the distribution can be given by calculating two bounds: $\Delta n_{10\%}$ such that 10% of the cells had net uptake greater than $\bar{n} + \Delta n_{10\%}$, and $\Delta n_{90\%}$ such that 90% of the cells had net uptake greater than $\bar{n} - \Delta n_{90\%}$. Using this notation, FITC-dextran uptake is characterized by $\bar{n}^{+\Delta n_{10\%}}_{-\Delta n_{90\%}} = 1.4^{+1.0}_{-1.28} \times 10^5$ molecules per cell. We emphasize that '$\pm$' does not indicate a measurement error, but instead a true distribution within the cell population.

FITC-dextran is relatively uncharged, is therefore relatively unaffected directly by electric fields and Born energy repulsion [16,17], and can be expected to be significantly transported by diffusion through pores. Models which correctly describe the electrical behavior of planar membranes have involved a rapidly changing pore population in which pores of many sizes are present [18,19]. In the case of electroporation causing significant molecular transport, membrane permeability increases dramatically as pores rapidly expand [6,7]. In cell membranes some large pores may become 'trapped' through interaction with membrane proteins and other cell constituents, resulting in a persistent high permeability. Subsequently, during the membrane recovery phase, pores presumably shrink and disappear, so that the membrane permeability should exhibit progressively smaller molecular cutoffs. Measurements of the number of transported molecules, made after exposing cells to solutions of molecules at different times relative to a pulse should allow testing of such mechanisms.

The electroporative uptake of the much smaller PI molecule was much larger, even though PI was supplied at a lower concentration (80 μM), and the case for interpreting cell fluorescence as uptake is even stronger. Three histograms of RF, calibrated in terms of numbers of bound PI, are of interest: unpulsed cells, methanol-fixed cells, and pulsed cells (figs 1 and 3). For unpulsed cells the small amount of RF per cell is consistent with negligible PI binding, as is well established in the use of PI as a membrane integrity stain in dye exclusion tests [11,13]. We interpret the small non-zero RF signal as originating from the 80 μM soluble PI which is extracellular, and whose weak RF is measured when a RBS trigger signal is generated by a cell. The use of a large number of methanol-fixed cells provides a calibration. Cells grown and harvested in the same way as pulsed cells are fixed and exposed to PI in solution. The fixed, highly fluorescent cells are then analyzed by flow cytometry, serving as a statistically large number (e.g. 10^4) of reference cells, for which the average RF was previously determined directly using fixed cells in the spectrofluorimeter. In this way, the fixed cells serve the same purpose as the GF beads: they are fluorescent particles capable of triggering the flow cytometer, and then being individually measured for fluorescence emission intensity. Unlike the tight distribution in amount of GF exhibited by the beads, there is a broad distribution in the amount of RF in a population of fixed cells. One might ob-

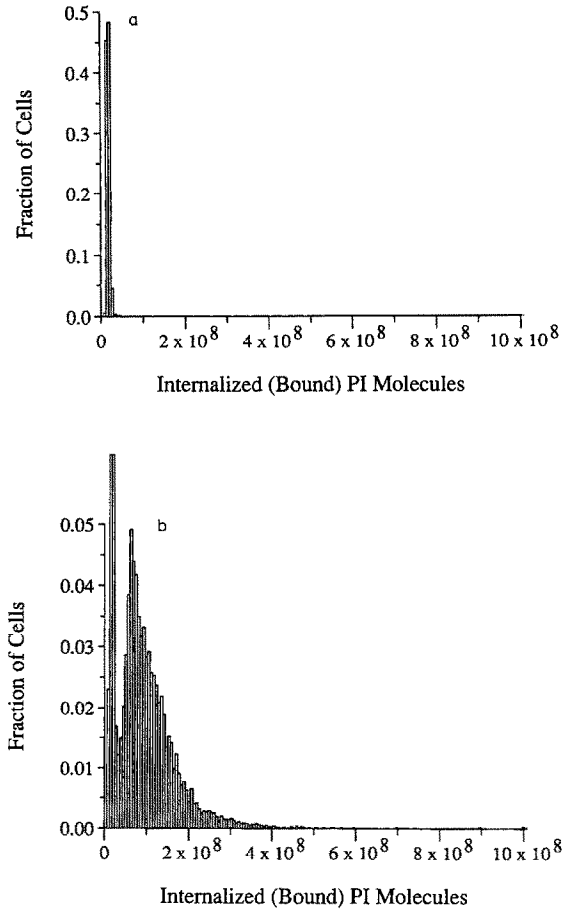

Fig.3. Results similar to those of fig.2, but for a much smaller propidium iodide (PI) molecule. (a) Control distribution obtained with unpulsed cells. (b) Pulsed population distribution of the number of PI molecules taken up by individual cells exposed throughout to a concentration of 80 μM for 5 min at E_e = 8 ± 0.5 kV/cm. This 16-fold higher (cf. fig.1) PI concentration was used to drive whatever transport mechanism operates because of electroporation, as the amount of uptake occurring with 5 μM was too small to obtain accurate measurements. The number of PI molecules is given in terms of the number of molecules bound to doubly stranded nucleic acids. Using the same notation as in fig.2, we found $\bar{n}_{-\Delta n90\%}^{+\Delta n10\%} = 1.0^{+0.71}_{-0.86} \times 10^8$ molecules per cell. Again, the '±' indicates a true population variation, not an experimental error.

ject that this distribution of measurements prevents calibration of intracellularly bound PI. However, the ability to make a large number of individual flow cytometer measurements followed by computer determination of the average RF of the individual measurements provides the basis for the calibration. Specifically, the spectrofluorimeter measures the average RF directly, while flow cytometer measurements indirectly determine average RF through computation, so that the two determinations can be compared, and thereby provide the needed calibration. It should be emphasized that this calibration approach rests on the use of large numbers of individual fixed cell measurements, which results in sufficiently accurate determinations of the average RF per fixed cell. As shown in fig.3, the electroporative uptake of PI is strikingly large, and also exhibits a distribution within the cell population. For the single pulse condition used, an average molecular uptake was $\bar{n}_{-\Delta n90\%}^{+\Delta n10\%} = 1.0^{+0.71}_{-0.86} \times 10^8$ molecules.

The propidium iodide experiments are significantly different from the dextran experiments in that the uptake of PI molecules involves their capture by intracellular binding sites (doubly stranded nucleic acids). A transient transport mechanism is indicated, because the number of internalized PI molecules is less than the number of intracellular binding sites for PI. More specifically, even with an extracellular PI concentration sixteen times that used with methanol-fixed cells, the number of molecules which entered and bound to intracellular sites was only 30% of the total number of accessible binding sites. Although electrokinetic transport may also occur during the short time that large fields exist, diffusion through pores should be a significant transport mechanism for a small molecule. The fact that significant intracellular binding occurs may provide a way to experimentally estimate the time integral of the rapidly changing membrane permeability to PI, as the intracellular soluble concentration of PI is held low by the intracellular binding. This approach can be extended to other molecular species (e.g. fluorescence-labeled antibodies) for which there is fairly strong intracellular binding. In this regard, it is noteworthy that the electroporative uptake of antibodies by intact yeast, and their subsequent specific intracellular binding, has recently been reported [20]. If the strength and number of binding sites is large, the uptake process can be represented by the combination of a permeability and the binding sites. The permeability is a time varying barrier to entry, while the binding sites keep the intracellular soluble concentration low if the number of binding

sites is considerably larger than the number of molecules entering the cell. This is in contrast to the uptake of FITC-dextran, which presumably resides unbound within the cell following uptake.

In summary, we describe a quantitative method for measuring the population distribution of the number of molecules taken up by individual cells due to electroporation. This method should be generally applicable to vesicles and cells, and therefore be useful for both assisting optimization of electroporation applications and testing models of electroporative transport. Under our conditions, there were large numbers (on the order of 10^5) of molecules of an approximately electrically neutral macromolecule taken up, and still larger numbers (on the order of 10^8) of a small, polar molecule. Finally, a broad distribution of net molecular uptake within the cell population was found for both molecules.

Acknowledgements: We thank K.T. Powell, S.H. Grund, J.G. Bliss and A. Barnett for stimulating discussions. This study was supported by NIH (GM34077), the Army Research Office (Contract DAAG29-85-K-0241), and the DoD-University Research Instrumentation Program (Grant DAAG29-84-G-0066).

REFERENCES

[1] Zimmermann, U. (1986) Rev. Physiol. Biochem. Pharmacol. 105, 175–256.
[2] Neumann, E., Sowers, A. and Jordan, C. (1989) Electroporation and Electrofusion in Cell Biology, Plenum, New York.
[3] Neumann, E. and Rosenheck, K. (1972) J. Membr. Biol. 10, 279–290.
[4] Zimmermann, U., Pilwat, G. and Riemann, F. (1975) Biochim. Biophys. Acta 375, 209–219.
[5] Kinosita, K., jr and Tsong, T.Y. (1977) Nature 268, 438–441.
[6] Mehrle, W., Zimmermann, U. and Hampp, R. (1985) FEBS Lett. 185, 89–94.
[7] Sowers, A.E. and Lieber, M.R. (1986) FEBS Lett. 205, 179–184.
[8] Potter, H. (1988) Anal. Biochem. 174, 361–373.
[9] Zimmermann, U., Riemann, F. and Pilwat, G. (1976) Biochim. Biophys. Acta 436, 460–474.
[10] Weaver, J.C., Harrison, G.I., Bliss, J.G., Mourant, J.R. and Powell, K.T. (1988) FEBS Lett. 229, 30–34.
[11] Shapiro, H.M. (1988) Practical Flow Cytometry, Second Edition, A.R. Liss, New York.
[12] Bartoletti, D.C. (1989) MS Thesis, Massachusetts Institute of Technology.
[13] Jones, K.H. and Senft, J.A. (1985) Histochem. Cytochem. 33, 77–79.
[14] Bliss, J.G., Harrison, G.I., Mourant, J.R., Powell, K.T. and Weaver, J.C. (1988) Bioelectrochem. Bioenerget. 19, 57–71.
[15] Gray, M.L., Hoffman, R.A. and Hansen, W.P. (1983) Cytometry 3, 428–434.
[16] Weaver, J.C., Mintzer, R.A., Ling, H. and Sloan, S.R. (1986) Bioelectrochem. Bioelectroenerg. 15, 229–241.
[17] Weaver, J.C. and Powell, K.T. (1989) in: Electroporation and Electrofusion in Cell Biology (Neumann, E. et al. eds) pp.111–126, Plenum, New York.
[18] Powell, K.T., Derrick, E.G. and Weaver, J.C. (1986) Bioelectrochem. Bioelectroenerg. 15, 243–255.
[19] Barnett, A.S. and Weaver, J.C., submitted.
[20] Uno, I., Fukami, K., Kato, H., Takenwa, T. and Ishikawa, T. (1988) Nature 333, 188–190.